ACS Medicinal Chemistry Letters

pubs.acs.org/acsmedchemlett

Letter

Discovery of Pyridone-Substituted Triazolopyrimidine Dual A_{2A}/A_1 AR Antagonists for the Treatment of Ischemic Stroke

Mei-Lin Tang,[§] Zi-Hao Wen,[§] Jing-Huan Wang,[§] Mei-Ling Wang, Heyanhao Zhang, Xin-Hua Liu, Lin Jin,* and Jun Chang*

Cite This: *ACS Med. Chem. Lett.* 2022, 13, 436−442

Read Online

ACCESS | Metrics & More | Article Recommendations | Supporting Information

ABSTRACT: Ischemic stroke is a complex systemic disease characterized by high morbidity, disability, and mortality. The activation of the presynaptic adenosine A_{2A} and A_1 receptors modifies a variety of brain insults from excitotoxicity to stroke. Therefore, the discovery of dual A_{2A}/A_1 adenosine receptor (AR)-targeting therapeutic compounds could be a strategy for the treatment of ischemic stroke. Inspired by two clinical phase III drugs, ASP-5854 (dual A_{2A}/A_1 AR antagonist) and preladenant (selective A_{2A} AR antagonist), and using the hybrid medicinal strategy, we characterized novel pyridone-substituted triazolopyrimidine scaffolds as dual A_{2A}/A_1 AR antagonists. Among them, compound **1a** exerted excellent A_{2A}/A_1 AR binding affinity (K_i = 5.58/24.2 nM), an antagonistic effect (IC_{50} = 5.72/25.9 nM), and good metabolic stability in human liver microsomes, rat liver microsomes, and dog liver microsomes. Importantly, compound **1a** demonstrated a dose−effect relationship in the oxygen-glucose deprivation/reperfusion (OGD/R)-treated HT22 cell model. These findings support the development of dual A_{2A}/A_1 AR antagonists as a potential treatment for ischemic stroke.

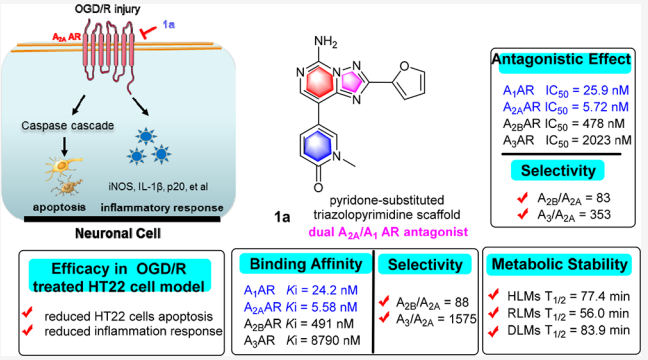

KEYWORDS: *Ischemic stroke, dual A_{2A}/A_1 AR antagonist, pyridone-substituted triazolopyrimidine*

Adenosine, the naturally occurring purine nucleoside, acts as an endogenous modulator in both the central and peripheral nervous systems by interacting with four subtypes of specific G-protein-coupled receptors (GPCRs): A_1, A_{2A}, A_{2B}, and A_3 adenosine receptors (ARs). The A_1 and A_3 ARs are negatively coupled to adenylyl cyclase and exert an inhibitory effect on cyclic adenosine monophosphate (cAMP) production by recruiting the G_i protein, whereas the A_{2A} and A_{2B} ARs promote adenylyl cyclase activation and subsequent cAMP production by recruiting the G_s protein.[1−4] The A_{2A} and A_1 ARs are highly enriched in specific parts of the central nervous system (CNS) and are associated with motor activity, psychiatric behaviors, and neuronal cell death. Many potent selective A_{2A} AR antagonists have been designed as promising candidates for their beneficial effects on Parkinson's disease (PD),[5] ischemia,[6] epilepsy,[7] Huntington's disease (HD),[8] and Alzheimer's disease (AD).[9]

Over the past three decades, the search for novel A_{2A} AR antagonists has been greatly expanded, and a large number of drug candidates have entered clinical trials (Figure 1). Unfortunately, only istradefylline (KW-6002) has been licensed as an antiparkinsonian drug in Japan (2013) and the United States (2019);[10] other A_{2A} AR antagonists (preladenant,[11] vipadenant,[12] tozadenant,[13] etc.) were terminated because of a lack of efficacy *in vivo* or toxicity.[14] Recently,

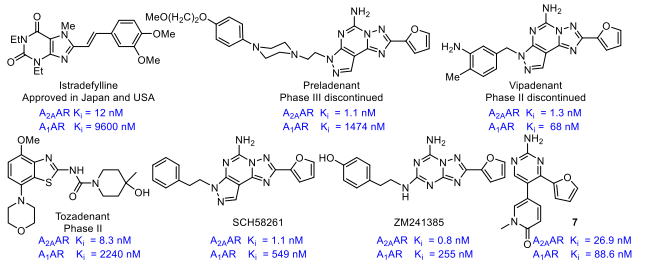

Figure 1. Reported selective A_{2A} and dual A_{2A}/A_1 AR antagonists.

the A_{2A} AR emerged as a novel immune checkpoint for the development of a cancer immunotherapy drug in combination with PD-1/PD-L1 or anti-CTLA-4 monoclonal antibody (mAb).[15,16] ZM241385 significantly inhibited tumor growth in a lung metastasis model and induced a remarkable delay in tumor growth in melanoma-bearing mice when combined with

Received: October 29, 2021
Accepted: February 16, 2022
Published: February 21, 2022

anti-CTLA-4 mAb.[17,18] Moreover, the discovery and development of dual A_x AR therapeutic compounds is an attractive and alternative therapeutic strategy for improving the *in vivo* efficacy of a single target. For example, AB928, a potent and selective dual A_{2A}/A_{2B} AR antagonist discovered by Arcus Biosciences, is currently undergoing clinical trials in multiple cancer settings.[19,20]

Ischemic stroke is a complex systemic disease characterized by high morbidity, disability, and mortality.[21] Increasing substantial evidence has shown a protective role for A_{2A} AR antagonists in striatal and nigral neurons through the prevention of glutamate-dependent neuronal death, thereby reducing cortical damage in a variety of ischemic stroke models.[22−24] In A_{2A} AR knockout (KO) mice, transient focal ischemia causes less neuronal damage compared with that in wild-type (WT) mice. The selective A_{2A} AR antagonist SCH58261 reduced ischemic brain damage in an adult rat model of focal cerebral ischemia.[25−27] Meanwhile, the activation of the A_1 AR was able to induce ischemic damage protection and the reduction of both reactive and proliferative microglia/macrophages after experimental stroke in rats.[28,29] These results demonstrate that the activation of the presynaptic A_{2A} and A_1 ARs modifies a variety of brain insults from excitotoxicity to stroke.

Owing to our interest in ARs and the field of ischemic stroke, we set out to design and synthesize novel dual A_{2A}/A_1 AR antagonists based on the crystal structures of A_{2A} AR (PDB: 3EML) and A_1 AR (PDB: 5EUN) complexes.[30,31] We herein report the discovery and characterization of a new chemotype of dual A_{2A}/A_1 AR antagonists with a pyridone-substituted triazolopyrimidine scaffold, in which compound **1a** demonstrated a remarkable dose−effect relationship in the oxygen-glucose deprivation/reperfusion (OGD/R)-treated HT22 cell model.

Our initial design was inspired by two known clinical phase III drug candidates, preladenant (selective A_{2A} AR antagonist), with a triazolopyrimidine scaffold,[11] and ASP-5854 (dual A_{2A}/A_1 AR antagonist), with a pyrazine scaffold[32] (Figure 2). Using insight from preladenant cocrystal structures with an A_{2A} AR and an A_1 AR, we noticed that the primary amide (ring A) and the triazole (ring B) with furan rings in preladenant established two bidentate hydrogen-bonding interactions with Glu169 and Asn253 (Figure 2A,B) with similar binding modes. However, preladenant is just a selective A_{2A} AR antagonist, suggesting that the triazolopyrimidine scaffold was a key pharmacophore as the selective A_{2A} AR antagonist. The primary amide in ASP-5854 also formed a bidentate hydrogen-bonding interaction with Asn253, in which the A_{2A} AR was the key pharmacophore. Moreover, the pyridone in ASP-5854 formed an additional hydrogen bond with His278 in the A_{2A} AR. By contrast, when docked with A_1 AR, the pyridone in ASP-5854 formed a hydrogen bond with Thr90 in the A_1 AR, which may be a key pharmacophore as the A_1 AR antagonist. On the basis of these analyses, we intended to exploit the hybrid drug design approach to access all five aforementioned interactions with the goal of identifying a novel chemical scaffold dual A_{2A}/A_1 AR antagonist with better drug-like properties. Therefore, we designed and synthesized a series of compounds with the novel pyridone-substituted triazolopyrimidine chemotype and carried out a systematic study of structure−activity relationships (SARs).

As shown in Scheme 1, the synthetic strategy of **1a**−**1i** involved a three-step sequence, including a nucleophilic

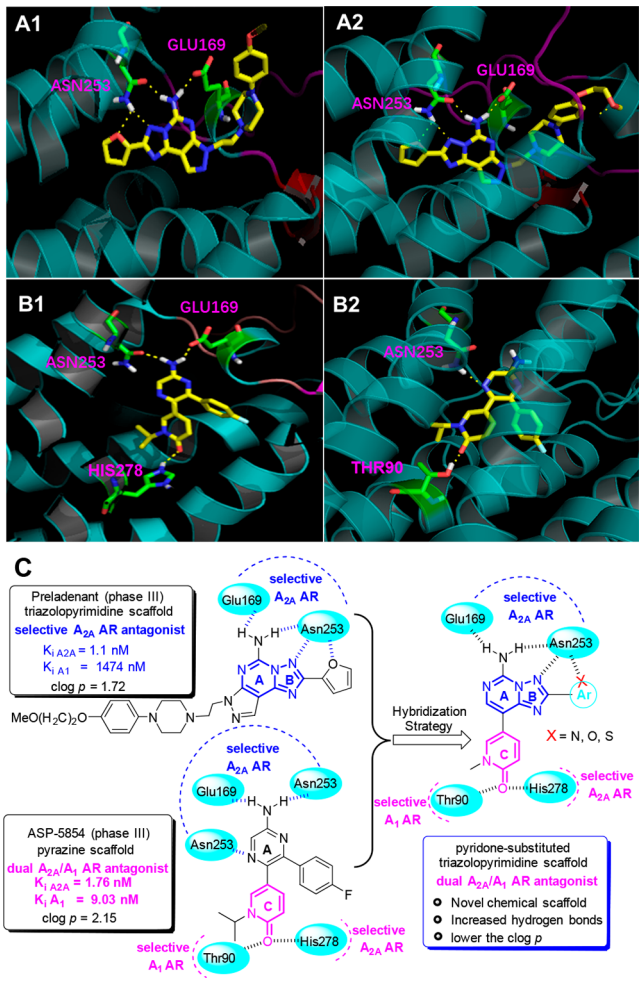

Figure 2. Design strategy of novel chemotype dual A_{2A}/A_1 AR antagonists. (A) Interactions shown between preladenant with A_{2A} AR (A1) and A_1 AR (A2). (B) Interactions shown between ASP-5854 with A_{2A} AR (B1) and A_1 AR (B2). (C) Hybridization strategy of novel pyridone-substituted triazolopyrimidine scaffold.

Scheme 1[a]

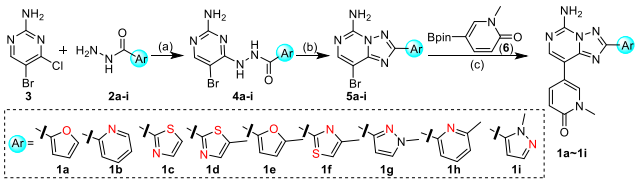

[a]Reagents and conditions: (a) *n*-BuOH, 120 °C, 8 h; (b) HMDS, BSA, 120 °C, 8 h; (c) $Pd(dppf)Cl_2$, K_2CO_3, dioxane, H_2O, 90 °C, 8 h, 4.1−6.5%, three steps.

substitution reaction, Dimroth rearrangement, and a Suzuki coupling process, starting from commercially available aryl formamide derivatives **2**. Initially, the nucleophilic substitution of 5-bromo-4-chloropyrimidin-2-amine (**3**) by aryl formamide **2a**−**2i** at 120 °C in *n*-butanol proceeded smoothly to deliver compounds **4a**−**4i**. The subsequent Dimroth rearrangement of compounds **4a**−**4i** was conducted in the presence of *N*,*O*-bis(trimethylsilyl) acetamide (BSA) and hexamethyldisilazane (HMDS) at 120 °C to give the desired cyclization triazolopyrimidine compounds **5a**−**5i**. Finally, compounds **5a**−**5i** were coupled to pyridone boronic esters (**6**) to afford

https://doi.org/10.1021/acsmedchemlett.1c00599
ACS Med. Chem. Lett. 2022, 13, 436−442

Table 1. Binding Affinity (K_i, nM) of Compounds 1a−1i at the Adenosine Receptors

compound	binding affinity (K_i, nM)			
	A_1 AR	A_{2A} AR	A_{2B} AR	A_3 AR
1a	24.2 ± 5.49	5.58 ± 0.11	491 ± 4.45	8790 ± 3.27
1b	37.6 ± 4.34	62.4 ± 3.43	>10000	>10000
1c	78.0 ± 6.75	84.6 ± 4.73	1586 ± 4.14	>10000
1d	21.9 ± 4.53	43.9 ± 2.75	9919 ± 6.56	2934 ± 4.11
1e	88.4 ± 6.36	448 ± 4.42	>10000	2964 ± 4.55
1f	926 ± 3.70	1032 ± 2.46	>10000	>10000
1g	722 ± 9.90	3427 ± 4.20	>10000	>10000
1h	1719 ± 6.12	3767 ± 2.41	>10000	>10000
1i	2973 ± 4.65	797 ± 2.44	>10000	>10000
7	88.6 ± 5.56	26.9 ± 2.71	58.9 ± 3.33	>10000

the final products **1a−1i** in an acceptable yield (4.1−6.5%) over three steps.

The binding affinity of the synthesized pyridone-substituted triazolopyrimidine derivatives (**1a−1i**) toward the A_{2A} and A_1 ARs, along with A_{2B} and A_3 ARs, was evaluated in competitive binding experiments using membrane preparation of the human recombinants A_1, A_{2A} and A_3, and the A_{2B} AR overexpressed from CHO, HeLa, and HEK-293 cells, respectively. [^{3}H] DPCPX (A_1), [^{3}H]ZM241385 (A_{2A}), [^{3}H]DPCPX (A_{2B}), and [^{3}H]NECA (A_3) were used as radioligands.[33] The binding affinity data of synthesized compounds are listed in Table 1, with pyrazine antagonist compound **7** chosen as the reference. Among them, compound **1a** with a furan ring as the Ar group exhibited the most excellent binding affinity with a K_i value of 5.58 nM against the A_{2A} AR and 24.2 nM against the A_1 AR and a high degree of selectivity for the A_{2B} AR (A_{2B}/A_{2A} 88-fold) and the A_3 AR (A_3/A_{2A} 1575-fold), respectively. Compounds **1b** (pyridine as the Ar group) and **1c** (thiazole as the Ar group) showed moderate binding affinity against the A_{2A} AR (K_i = 62.4 nM) and comparable binding activity against the A_1 AR (K_i = 84.6 nM), along with good selectivity over the A_{2B} and A_3 ARs. Interestingly, compound **1d** (5-methylthiazole as the Ar group) displayed the most potent binding affinity data, with a K_i value of 21.9 nM against the A_1 AR and two-fold selectivity over the A_{2A} AR, which can be used as a lead for the further optimization of selective A_1 AR antagonists. However, compounds **1e−1i** showed less binding affinity against A_1 to A_3 ARs compared with compounds **1a−1d** because of the introduction of a methyl group beside the heteroatom, which may increase the steric hindrance and affect the binding to the target cavity of A_1 to A_3 ARs. These results suggested that the introduction of heteroatoms in the Ar group was crucial for binding to the A_{2A} AR and increased its affinity, and furan as the Ar group was the most potent. Conversely, the introduction of a methyl group beside the heteroatom on the Ar group was fatal for binding to the target due to the steric hindrance.

Furthermore, the calcium flux functional experiments were carried out to assess the antagonistic/agonistic activity of the most potent compound **1a** at the A_{2A} and A_1 ARs, along with A_{2B} and A_3 ARs.[34] The functional assay data IC_{50} for **1a** shown in Figure 3 indicated that the excellent antagonist activity of **1a** was consistent with its binding affinity, whereas the agonist activity of **1a** was negligible.

Many studies have proven that neuron apoptosis is involved in the pathological process of ischemia injury. Thus the OGD/R model (*in vitro* ischemic model) was used to damage HT22 cells to simulate ischemic injury to investigate the effect of A_{2A}/A_1 AR antagonist compound **1a** on HT22 cell damage.[35] First, we investigated the effect of compound **1a** on cell apoptosis induced by OGD/R. The results demonstrated that OGD/R significantly induced apoptosis of HT22 cells, and compound **1a** reversed, in a concentration-dependent manner, the up-regulation of pro-apoptotic genes such as cleaved caspase-3, cleaved caspase-9, cleaved PARP1, p53, and Bax in OGD/R-treated HT22 cells (Figure 4A). Notably, immunofluorescence analyses revealed that the antiapoptotic gene Bcl-2 staining was enhanced by compound **1a** (Figure 4B). Likewise, the mRNA expression in the apoptosis markers (p53, Bax, Bcl-2) was consistent with the protein expression (Figure 4C). These results provided support that compound **1a** protected against cell apoptosis.

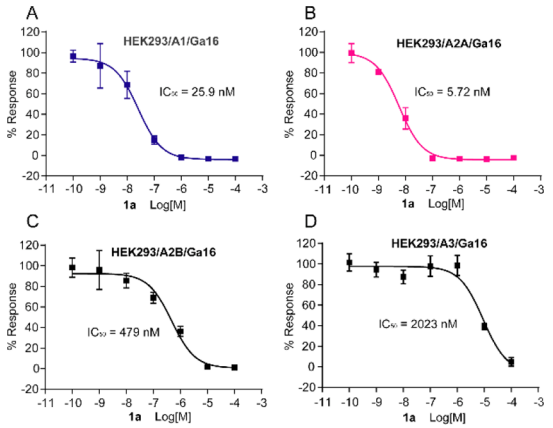

Figure 3. Antagonistic effect (IC_{50}, nM) of compound **1a** against A_1, A_{2A}, A_{2B}, and A_3 ARs.

Currently, there is strong evidence that inflammatory processes may contribute to secondary brain damage after ischemic stroke. Indeed, inflammation modulators including iNOS, COX-2, and VCAM-1 were induced by OGD/R; on the contrary, increased inflammation mediators were significantly inhibited by compound **1a** treatment (Figure 5A). Consistent with these findings, immunofluorescence staining revealed a lack of COX-2 in compound-**1a**-treated HT22 cells as compared with that in OGD/R-treated HT22 cells (Figure 5B). Recent findings identified that NLRP3 inflammasomes play a major role in neuronal cell death in stroke and further suggested that targeted inflammasome assembly and activity may ameliorate ischemic injury.[36,37] We found that OGD/R robustly induced the expression of inflammasome protein caspase-1 (p20) and mature pro-inflammatory cytokines IL-18

https://doi.org/10.1021/acsmedchemlett.1c00599
ACS Med. Chem. Lett. 2022, 13, 436−442

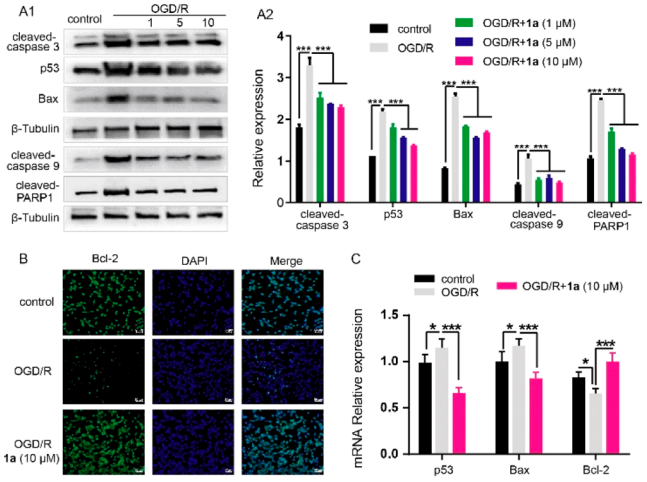

Figure 4. Compound **1a** prevented HT22 cell apoptosis after oxygen-glucose deprivation (OGD). (A) HT22 cells were pretreated with or without compound **1a** (1−10 μM) for 4 h and then were treated with OG, then 4 and 24 h of reoxygenation. Cell lysates were prepared and blotted with antibodies to Bax, p53, cleaved PARP1, cleaved caspase-3, and cleaved caspase-9; ***p < 0.001, all data are presented as the mean ± SD of three independent experiments. (B) HT22 cells were pretreated with or without 10 μM compound **1a** for 4 h and then were treated with OGD, then 4 and 24 h of reoxygenation. Cells were immunostained with antibody Bcl-2 (magnification, 200×). (C) HT22 cells were pretreated with or without 10 μM compound **1a** for 4 h and then were treated with OGD, then 4 and 24 h of reoxygenation. mRNA levels of Bax, p53, and Bcl2 were quantified using qRT-PCR. *p < 0.05, ***p < 0.001. All data are presented as the mean ± SD of three independent experiments.

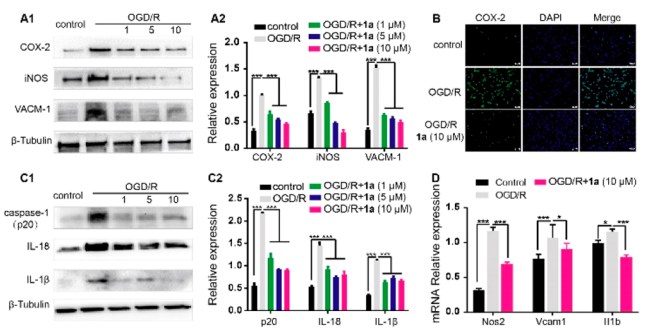

Figure 5. Compound **1a** reduced the inflammation response in OGD/R-treated HT22 cells. (A) HT22 cells were pretreated with or without compound **1a** (1−10 μM) for 4 h and then were treated with OGD, then 4 and 24 h of reoxygenation. Cell lysates were prepared and blotted with antibodies to iNOS, VCAM-1, and COX-2. ***p < 0.001. All data are presented as the mean ± SD of three independent experiments. (B) HT22 cells were pretreated with or without 10 μM compound **1a** for 4 h and then were treated with OGD, then 4 and 24 h of reoxygenation. Cells were immunostained with antibody COX-2 (magnification, 200×). (C) HT22 cells were pretreated with or without compound **1a** (1−10 μM) for 4 h and then were treated with OGD, then 4 and 24 h of reoxygenation. Cell lysates were prepared and blotted with antibodies to IL-1β, IL-18, and caspase-1 (p20). ***p < 0.001. All data are presented as the mean ± SD of three independent experiments. (D) HT22 cells were pretreated with or without 10 μM compound **1a** for 4 h and then were treated with OGD, then 4 and 24 h of reoxygenation. mRNA levels of Nos2, Vcam-1, and Il1b were quantified using qRT-PCR. *p < 0.05, ***p < 0.001. All data are presented as the mean ± SD of three independent experiments.

and IL-1β in HT22 cells; in turn, compound **1a** reduced caspase-1 (p20), IL-18, and IL-1β expression (Figure 5C). Likewise, the mRNA expression in inflammation markers Nos2, Vcam-1, and Il1b was consistent with the protein expression (Figure 5D). These results provide further support that compound **1a** protected against neuron OGD/R injury.

The metabolic stability is a prime consideration when developing a candidate (Table 2). The *in vitro* metabolic stability of compound **1a** was measured using human liver microsomes (HLMs), rat liver microsomes (RLMs), mouse liver microsomes (MsLMs), dog liver microsomes (DLMs), and monkey liver microsomes (MkLMs). Compound **1a** displayed good metabolic stability with a half life of 77.4, 56.0, and 83.9 min along with an intrinsic clearance (CL) of 16.1, 44.5, and 23.8 mL/min/kg in the HLMs, RLMs, and DLMs, respectively. After 60 min, 58.3, 48.6, and 60.6% of compound **1a** remained in the HLMs, RLMs, and DLMs, respectively. However, compound **1a** displayed less metabolic stability with a half life of 3.4 and 14.6 min along with an intrinsic clearance (CL) of 1601.7 and 128 mL/min/kg in the MsLMs and MkLMs, respectively. In addition, compound **1a** showed moderate brain penetration (B/P ratio = 0.22) (Table S3), which is suitable for the lead compound of ischemic stroke.

Table 2. *In Vitro* Metabolic Stability of Compound 1a in the Presence of Different Microsomes

parameters	$T_{1/2}$ (min)	$CL_{int(mic)}$ (μL/min/mg)	$CL_{int(liver)}$ (mL/min/kg)	unchanged (T = 1 h, %)
HLMs[a]	77.4	17.9	16.1	58.3
RLMs[b]	56.0	24.7	44.5	48.6
MsLMs[c]	3.4	404.5	1601.7	0.00
DLMs[d]	83.9	16.5	23.8	60.6
MkLMs[e]	14.6	94.8	128.0	5.9

[a]Human liver microsomes. [b]Rat liver microsomes. [c]Mouse liver microsomes. [d]Dog liver microsomes. [e]Monkey liver microsomes.

Molecular docking modeling was performed to interpret the dual A_{2A}/A_1 AR binding affinity of compound **1a** at the molecular level. The binding modes of compound **1a** at the A_{2A} and A_1 AR cavities were analyzed by docking simulations using the Autodock software package, with the crystal structures of the A_{2A} and A_1 AR complexes as templates, respectively. The docking results (Figure 6) revealed that compound **1a** adopted the general binding mode at both the A_{2A} and A_1 AR binding sites. In this binding mode, the pyridone-substituted triazolopyrimidine scaffold was positioned in the depth of the binding pocket and underwent a p−p interaction with the Phe residue (Phe168 in the A_{2A} AR,

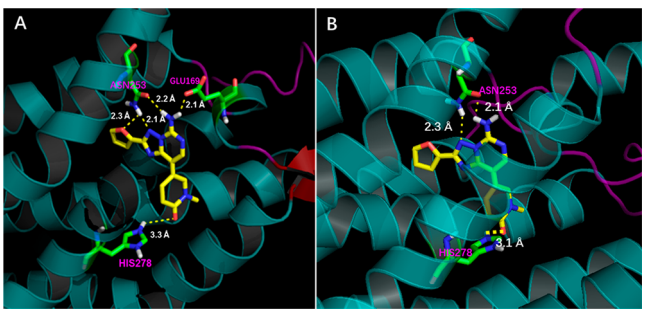

Figure 6. Schematic description of the ligand−target interaction between compound **1a** and (A) the A_{2A} AR and (B) the A_1 AR.

https://doi.org/10.1021/acsmedchemlett.1c00599
ACS Med. Chem. Lett. 2022, 13, 436−442

Phe171 in the A_1 AR). In addition, compound **1a** formed five hydrogen bonds with the A_{2A} AR (Glu169, Asn253, and His278), whereas it formed only two hydrogen bonds with the A_1 AR (Asn253). Therefore, compound **1a** adopted a much more favorable binding pose at the A_{2A} AR cavity than at the A_1 AR cavity. Moreover, the Autodock docking results also indicated that the binding pose was associated with a better docking score at the A_{2A} AR (−9.02 kcal/mol, K_i = 0.24 μM) than at the A_1 AR (−7.79 kcal/mol, K_i = 1.94 μM). Hence, the molecular docking results explained the A_{2A} AR affinity and the slight selectivity over the A_1 AR (4.4-fold) of compound **1a**.

In the present study, we designed and synthesized a novel pyridone-substituted triazolopyrimidine scaffold dual A_{2A}/A_1 AR antagonist using a computer-aided rational drug design approach along with a hybrid medicinal strategy, inspired by two phase III drugs, ASP-5854 (dual A_{2A}/A_1 AR antagonist) and preladenant (selective A_{2A} AR atagonist). *In vitro* evaluations of the A_1, A_{2A}, A_{2B}, and A_3 AR binding assays for the synthesized compounds showed promising results. Among them, compared with ASP-5854, the most potent compound **1a** showed a better clog *P* and comparable A_{2A}/A_1 AR binding affinity (K_i = 5.58/24.15 nM). In addition, compound **1a** showed excellent solubility at pH 1.2 (1.99 mg/mL), which is suitable for oral administration after some rational modification. Moreover, compound **1a** showed an excellent antagonistic effect (IC_{50} = 5.72/25.93 nM), moderate brain penetration (B/P ratio = 0.22), and good metabolic stability with $T_{1/2HLMs}$ = 77.4 min, $T_{1/2RLMs}$ = 56 min and $T_{1/2DLMs}$ = 83.9 min. Importantly, compound **1a** demonstrated a remarkable dose−effect relationship in the OGD/R-treated HT22 cell model, including the reduction of HT22 cells apoptosis and an alleviation of inflammatory modulator (iNOS, COX-2, and VCAM-1) and inflammatory cytokine (p20, IL-18, IL-1β, Nos2, Vcam-1, and II1b) release. With these encouraging results, we anticipate that this novel pyridone-substituted triazolopyrimidine scaffold could be an excellent starting point for the further development of dual A_{2A}/A_1 AR antagonists to benefit the field of ischemic stroke. The current effort is focused on further improving the potency along with good pharmacokinetics and pharmacodynamics both *in vivo* and *in vitro*, and these findings will be reported in due course.

■ ASSOCIATED CONTENT

Supporting Information

The Supporting Information is available free of charge at https://pubs.acs.org/doi/10.1021/acsmedchemlett.1c00599.

Experimental procedures and characterization for all final compounds and descriptions of in vitro studies (PDF)

■ AUTHOR INFORMATION

Corresponding Authors

Jun Chang − *School of Pharmacy, Human Phenome Institute, Fudan University, Shanghai 201203, China;* orcid.org/0000-0001-6481-7130; Email: jchang@fudan.edu.cn

Lin Jin − *Department of Anesthesia, Zhongshan Hospital, Fudan University, Shanghai 200032, China*; Email: jin.lin@zs-hospital.sh.cn

Authors

Mei-Lin Tang − *School of Pharmacy, Human Phenome Institute, Fudan University, Shanghai 201203, China*

Zi-Hao Wen − *School of Pharmacy, Human Phenome Institute, Fudan University, Shanghai 201203, China*

Jing-Huan Wang − *School of Pharmacy, Human Phenome Institute, Fudan University, Shanghai 201203, China*

Mei-Ling Wang − *School of Pharmacy, Human Phenome Institute, Fudan University, Shanghai 201203, China*

Heyanhao Zhang − *School of Pharmacy, Human Phenome Institute, Fudan University, Shanghai 201203, China*

Xin-Hua Liu − *School of Pharmacy, Human Phenome Institute, Fudan University, Shanghai 201203, China*

Complete contact information is available at: https://pubs.acs.org/10.1021/acsmedchemlett.1c00599

Author Contributions

[§]M.-L.T., Z.-H.W., and J.-H.W. contributed equally.

Funding

This project was supported financially by the National Natural Science Foundation of China (81803605, 81903422) and the Science and Technology Commission of Shanghai Municipality (18431900600).

Notes

The authors declare no competing financial interest.

■ ACKNOWLEDGMENTS

We also thank Prof. Xin Xie (Shanghai Institute of Materia Medica, Chinese Academy of Science) for the calcium flux functional experiments.

■ ABBREVIATIONS

AR, adenosine receptor; OGD/R, oxygen-glucose deprivation/reperfusion; iNOS, inducible nitric oxide synthase; COX-2, cyclooxygenase 2; VCAM-1, vascular cell adhesion molecule 1; p20, protein 20; IL-18, interleukin-18; IL-1β, interleukin-1β; Nos2, nitric oxide synthase 2; GPCR, G-protein-coupled receptor; cAMP, cyclic adenosine monophosphate; PD, Parkinson's disease; HD, Huntington's disease; AD, Alzheimer's disease; KO, knockout; WT, wild-type; SAR, structure−activity relationship; BSA, *N*,*O*-bis(trimethylsilyl) acetamide; HMDS, hexamethyldisilazane; NLRP3, NLR family pyrin domain containing 3; HLM, human liver microsome; RLM, rat liver microsome; MsLM, mouse liver microsome; DLM, dog liver microsome; MkLM, monkey liver microsome; CL, clearance

■ REFERENCES

(1) Layland, J.; Carrick, D.; Lee, M.; Oldroyd, K.; Berry, C. Adenosine: physiology, pharmacology, and clinical applications. *JACC Cardiovasc. Interv.* **2014**, *7*, 581−591.

(2) Lee, Y.; Hou, X.; Lee, J. H.; Nayak, A.; Alexander, V.; Sharma, P. K.; Chang, H.; Phan, K.; Gao, Z. G.; Jacobson, K. A.; Choi, S.; Jeong, L. S. Subtle Chemical Changes Cross the Boundary between Agonist and Antagonist: New A(3) Adenosine Receptor Homology Models and Structural Network Analysis Can Predict This Boundary. *J. Med. Chem.* **2021**, *64*, 12525−12536.

(3) Liu, Y. J.; Chen, J.; Li, X.; Zhou, X.; Hu, Y. M.; Chu, S. F.; Peng, Y.; Chen, N. H. Research progress on adenosine in central nervous system diseases. *CNS Neurosci. Ther.* **2019**, *25*, 899−910.

(4) Effendi, W. I.; Nagano, T.; Kobayashi, K.; Nishimura, Y. Focusing on Adenosine Receptors as a Potential Targeted Therapy in Human Diseases. *Cells* **2020**, *9*, 785.

(5) (a) Shook, B. C.; Jackson, P. F. Adenosine A(2A) Receptor Antagonists and Parkinson's Disease. *ACS Chem. Neurosci.* **2011**, *2*, 555−567. (b) Zheng, J.; Zhang, X.; Zhen, X. Development of Adenosine A(2A) Receptor Antagonists for the Treatment of Parkinson's Disease: A Recent Update and Challenge. *ACS Chem. Neurosci.* **2019**, *10*, 783−791. (c) Hagenow, S.; Affini, A.; Pioli, E. Y.; Hinz, S.; Zhao, Y.; Porras, G.; Namasivayam, V.; Müller, C. E.; Lin, J. S.; Bezard, E.; Stark, H. Adenosine A(2A)R/A(1)R Antagonists Enabling Additional H(3)R Antagonism for the Treatment of Parkinson's Disease. *J. Med. Chem.* **2021**, *64*, 8246−8262. (d) Kim, A.; Lalonde, K.; Truesdell, A.; Gomes Welter, P.; Brocardo, P. S.; Rosenstock, T. R.; Gil-Mohapel, J. New Avenues for the Treatment of Huntington's Disease. *Int. J. Mol. Sci.* **2021**, *22*, 8363. (e) Basu, S.; Barawkar, D. A.; Ramdas, V.; Naykodi, M.; Shejul, Y. D.; Patel, M.; Thorat, S.; Panmand, A.; Kashinath, K.; Bonagiri, R.; Prasad, V.; Bhat, G.; Quraishi, A.; Chaudhary, S.; Magdum, A.; Meru, A. V.; Ghosh, I.; Bhamidipati, R. K.; Raje, A. A.; Madgula, V. L. M.; De, S.; Rouduri, S. R.; Palle, V. P.; Chugh, A.; Hariharan, N.; Mookhtiar, K. A. Discovery of Potent and Selective A(2A) Antagonists with Efficacy in Animal Models of Parkinson's Disease and Depression. *ACS Med. Chem. Lett.* **2017**, *8*, 835−840.

(6) (a) Ganesana, M.; Venton, B. J. Early changes in transient adenosine during cerebral ischemia and reperfusion injury. *PLoS One* **2018**, *13*, No. e0196932. (b) Wang, Y.; Venton, B. J. Caffeine Modulates Spontaneous Adenosine and Oxygen Changes during Ischemia and Reperfusion. *ACS. Chem. Neurosci.* **2019**, *10*, 1941−1949.

(7) (a) Boison, D.; Rho, J. M. Epigenetics and epilepsy prevention: The therapeutic potential of adenosine and metabolic therapies. *Neuropharmacology* **2020**, *167*, 107741. (b) Tescarollo, F. C.; Rombo, D. M.; DeLiberto, L. K.; Fedele, D. E.; Alharfoush, E.; Tomé, R.; Cunha, R. A.; Sebastião, A. M.; Boison, D. Role of Adenosine in Epilepsy and Seizures. *J. Caffeine Adenosine Res.* **2020**, *10*, 45−60.

(8) (a) Blum, D.; Chern, Y.; Domenici, M. R.; Buée, L.; Lin, C. Y.; Rea, W.; Ferré, S.; Popoli, P. The Role of Adenosine Tone and Adenosine Receptors in Huntington's Disease. *J. Caffeine Adenosine Res.* **2018**, *8*, 43−58. (b) Huang, N. K.; Lin, J. H.; Lin, J. T.; Lin, C. I.; Liu, E. M.; Lin, C. J.; Chen, W. P.; Shen, Y. C.; Chen, H. M.; Chen, J. B.; Lai, H. L.; Yang, C. W.; Chiang, M. C.; Wu, Y. S.; Chang, C.; Chen, J. F.; Fang, J. M.; Lin, Y. L.; Chern, Y. A new drug design targeting the adenosinergic system for Huntington's disease. *PLoS One* **2011**, *6*, No. e20934.

(9) (a) Franco, R.; Rivas-Santisteban, R.; Casanovas, M.; Lillo, A.; Saura, C. A.; Navarro, G. Adenosine A(2A) Receptor Antagonists Affects NMDA Glutamate Receptor Function. Potential to Address Neurodegeneration in Alzheimer's Disease. *Cells* **2020**, *9*, 1075. (b) Gessi, S.; Poloni, T. E.; Negro, G.; Varani, K.; Pasquini, S.; Vincenzi, F.; Borea, P. A.; Merighi, S. A(2A) Adenosine Receptor as a Potential Biomarker and a Possible Therapeutic Target in Alzheimer's Disease. *Cells* **2021**, *10*, 2344.

(10) (a) Ishibashi, K.; Miura, Y.; Wagatsuma, K.; Toyohara, J.; Ishiwata, K.; Ishii, K. Adenosine A(2A) Receptor Occupancy by Long-Term Istradefylline Administration in Parkinson's Disease. *Mov. Disord.* **2021**, *36*, 268−269. (b) Hattori, N.; Kitabayashi, H.; Kanda, T.; Nomura, T.; Toyama, K.; Mori, A. A Pooled Analysis From Phase 2b and 3 Studies in Japan of Istradefylline in Parkinson's Disease. *Mov. Disord.* **2020**, *35*, 1481−1487.

(11) Yuan, G.; Jankins, T. C.; Patrick, C. G., Jr.; Philbrook, P.; Sears, O.; Hatfield, S.; Sitkovsky, M.; Vasdev, N.; Liang, S. H.; Ondrechen, M. J.; Pollastri, M. P.; Jones, G. B. Fluorinated Adenosine A(2A) Receptor Antagonists Inspired by Preladenant as Potential Cancer Immunotherapeutics. *Int. J. Med. Chem.* **2017**, *2017*, 1−8.

(12) Shin, S. H.; Park, M. H.; Byeon, J. J.; Lee, B. I.; Park, Y.; Kim, N.; Choi, J.; Shin, Y. G. Analysis of Vipadenant and Its In Vitro and In Vivo Metabolites via Liquid Chromatography-Quadrupole-Time-of-Flight Mass Spectrometry. *Pharmaceutics* **2018**, *10*, 260.

(13) Lee, B. I.; Park, M. H.; Shin, S. H.; Byeon, J. J.; Park, Y.; Kim, N.; Choi, J.; Shin, Y. G. Quantitative Analysis of Tozadenant Using Liquid Chromatography-Mass Spectrometric Method in Rat Plasma and Its Human Pharmacokinetics Prediction Using Physiologically Based Pharmacokinetic Modeling. *Molecules* **2019**, *24*, 1295.

(14) Shah, U.; Hodgson, R. Recent progress in the discovery of adenosine A(2A) receptor antagonists for the treatment of Parkinson's disease. *Curr. Opin. Drug Discovery Dev.* **2010**, *13*, 466−480.

(15) (a) Reddy, G. L.; Sarma, R.; Liu, S.; Huang, W.; Lei, J.; Fu, J.; Hu, W. Design, synthesis and biological evaluation of novel scaffold benzo[4,5]imidazo [1,2-a]pyrazin-1-amine: Towards adenosine A(2A) receptor (A(2A) AR) antagonist. *Eur. J. Med. Chem.* **2021**, *210*, 113040. (b) Vigano, S.; Alatzoglou, D.; Irving, M.; Ménétrier-Caux, C.; Caux, C.; Romero, P.; Coukos, G. Targeting Adenosine in Cancer Immunotherapy to Enhance T-Cell Function. *Front. Immunol.* **2019**, *10*, 925.

(16) Loi, S.; Pommey, S.; Haibe-Kains, B.; Beavis, P. A.; Darcy, P. K.; Smyth, M. J.; Stagg, J. CD73 promotes anthracycline resistance and poor prognosis in triple negative breast cancer. *Proc. Natl. Acad. Sci. U. S. A.* **2013**, *110*, 11091−11096.

(17) Ohta, A.; Gorelik, E.; Prasad, S. J.; Ronchese, F.; Lukashev, D.; Wong, M. K.; Huang, X.; Caldwell, S.; Liu, K.; Smith, P.; Chen, J. F.; Jackson, E. K.; Apasov, S.; Abrams, S.; Sitkovsky, M. A2A adenosine receptor protects tumors from antitumor T cells. *Proc. Natl. Acad. Sci. U. S. A.* **2006**, *103*, 13132−13137.

(18) Iannone, R.; Miele, L.; Maiolino, P.; Pinto, A.; Morello, S. Adenosine limits the therapeutic effectiveness of anti-CTLA4 mAb in a mouse melanoma model. *Am. J. Cancer. Res.* **2014**, *4*, 172−181.

(19) Seitz, L.; Jin, L.; Leleti, M.; Ashok, D.; Jeffrey, J.; Rieger, A.; Tiessen, R. G.; Arold, G.; Tan, J. B. L.; Powers, J. P.; Walters, M. J.; Karakunnel, J. Safety, tolerability, and pharmacology of AB928, a novel dual adenosine receptor antagonist, in a randomized, phase 1 study in healthy volunteers. *Invest New Drugs* **2019**, *37*, 711−721.

(20) Rosen, B. R.; Ul Sharif, E.; Miles, D. H.; Chan, N. S.; Leleti, M. R.; Powers, J. P. Improved synthesis of sterically encumbered heteroaromatic biaryls from aromatic b-keto esters. *Tetrahedron Lett.* **2020**, *61*, 151855.

(21) Hankey, G. J. Secondary stroke prevention. *Lancet Neurol* **2014**, *13*, 178−94.

(22) Gaudry, M.; Vairo, D.; Marlinge, M.; Gaubert, M.; Guiol, C.; Mottola, G.; Gariboldi, V.; Deharo, P.; Sadrin, S.; Maixent, J. M.; Fenouillet, E.; Ruf, J.; Guieu, R.; Paganelli, F. Adenosine and Its Receptors: An Expected Tool for the Diagnosis and Treatment of Coronary Artery and Ischemic Heart Diseases. *Int. J. Mol. Sci.* **2020**, *21*, 5321.

(23) Reiss, A. B.; Grossfeld, D.; Kasselman, L. J.; Renna, H. A.; Vernice, N. A.; Drewes, W.; Konig, J.; Carsons, S. E.; DeLeon, J. Adenosine and the Cardiovascular System. *Am. J. Cardiovasc. Drugs* **2019**, *19*, 449−464.

(24) Zhou, Y.; Zeng, X.; Li, G.; Yang, Q.; Xu, J.; Zhang, M.; Mao, X.; Cao, Y.; Wang, L.; Xu, Y.; Wang, Y.; Zhang, Y.; Xu, Z.; Wu, C.; Chen, J. F.; Hoda, M. N.; Liu, Z.; Hong, M.; Huo, Y. Inactivation of endothelial adenosine A(2A) receptors protects mice from cerebral ischaemia-induced brain injury. *Br. J. Pharmacol.* **2019**, *176*, 2250−2263.

(25) Melani, A.; Pantoni, L.; Bordoni, F.; Gianfriddo, M.; Bianchi, L.; Vannucchi, M. G.; Bertorelli, R.; Monopoli, A.; Pedata, F. The selective A2A receptor antagonist SCH 58261 reduces striatal transmitter outflow, turning behavior and ischemic brain damage induced by permanent focal ischemia in the rat. *Brain Res.* **2003**, *959*, 243−250.

(26) Melani, A.; Gianfriddo, M.; Vannucchi, M. G.; Cipriani, S.; Baraldi, P. G.; Giovannini, M. G.; Pedata, F. The selective A2A receptor antagonist SCH 58261 protects from neurological deficit, brain damage and activation of p38 MAPK in rat focal cerebral ischemia. *Brain Res.* **2006**, *1073−1074*, 470−480.

(27) Pedata, F.; Gianfriddo, M.; Turchi, D.; Melani, A. The protective effect of adenosine A2A receptor antagonism in cerebral ischemia. *Neurol. Res.* **2005**, *27*, 169−174.

(28) Chen, Z.; Xiong, C.; Pancyr, C.; Stockwell, J.; Walz, W.; Cayabyab, F. S. Prolonged adenosine A1 receptor activation in

https://doi.org/10.1021/acsmedchemlett.1c00599
ACS Med. Chem. Lett. 2022, 13, 436−442

hypoxia and pial vessel disruption focal cortical ischemia facilitates clathrin-mediated AMPA receptor endocytosis and long-lasting synaptic inhibition in rat hippocampal CA3-CA1 synapses: differential regulation of GluA2 and GluA1 subunits by p38 MAPK and JNK. *J. Neurosci.* **2014**, *34*, 9621−43.
(29) Joya, A.; Ardaya, M.; Montilla, A.; Garbizu, M.; Plaza-García, S.; Gómez-Vallejo, V.; Padro, D.; Gutiérrez, J. J.; Rios, X.; Ramos-Cabrer, P.; Cossío, U.; Pulagam, K. R.; Higuchi, M.; Domercq, M.; Cavaliere, F.; Matute, C.; Llop, J.; Martín, A. In vivo multimodal imaging of adenosine A(1) receptors in neuroinflammation after experimental stroke. *Theranostics* **2021**, *11*, 410−425.
(30) Jaakola, V. P.; Griffith, M. T.; Hanson, M. A.; Cherezov, V.; Chien, E. Y.; Lane, J. R.; Ijzerman, A. P.; Stevens, R. C. The 2.6 angstrom crystal structure of a human A2A adenosine receptor bound to an antagonist. *Science* **2008**, *322*, 1211−1217.
(31) Glukhova, A.; Thal, D. M.; Nguyen, A. T.; Vecchio, E. A.; Jörg, M.; Scammells, P. J.; May, L. T.; Sexton, P. M.; Christopoulos, A. Structure of the Adenosine A(1) Receptor Reveals the Basis for Subtype Selectivity. *Cell* **2017**, *168*, 867−877.
(32) Mihara, T.; Mihara, K.; Yarimizu, J.; Mitani, Y.; Matsuda, R.; Yamamoto, H.; Aoki, S.; Akahane, A.; Iwashita, A.; Matsuoka, N. Pharmacological characterization of a novel, potent adenosine A1 and A2A receptor dual antagonist, 5-[5-amino-3-(4-fluorophenyl)pyrazin-2-yl]-1-isopropylpyridone-2(1H)-one (ASP5854), in models of Parkinson's disease and cognition. *J. Pharmacol. Exp. Ther.* **2007**, *323*, 708−719.
(33) (a) El Maatougui, A.; Azuaje, J.; González-Gómez, M.; Miguez, G.; Crespo, A.; Carbajales, C.; Escalante, L.; García-Mera, X.; Gutiérrez- de-Terán, H.; Sotelo, E. Discovery of Potent and Highly Selective A2B Adenosine Receptor Antagonist Chemotypes. *J. Med. Chem.* **2016**, *59*, 1967−1983. (b) Basu, S.; Barawkar, D. A.; Thorat, S.; Shejul, Y. D.; Patel, M.; Naykodi, M.; Jain, V.; Salve, Y.; Prasad, V.; Chaudhary, S.; Ghosh, I.; Bhat, G.; Quraishi, A.; Patil, H.; Ansari, S.; Menon, S.; Unadkat, V.; Thakare, R.; Seervi, M. S.; Meru, A. V.; De, S.; Bhamidipati, R. K.; Rouduri, S. R.; Palle, V. P.; Chug, A.; Mookhtiar, K. A. Design, Synthesis of Novel, Potent, Selective, Orally Bioavailable Adenosine A(2A) Receptor Antagonists and Their Biological Evaluation. *J. Med. Chem.* **2017**, *60*, 681−694.
(34) Zhu, T.; Fang, L. Y.; Xie, X. Development of a universal high-throughput calcium assay for G-protein- coupled receptors with promiscuous G-protein Galpha15/16. *Acta Pharmacol Sin* **2008**, *29*, 507−16.
(35) Wang, J.; Zhong, W.; Su, H.; Xu, J.; Yang, D.; Liu, X.; Zhu, Y. Histone methyltransferase Dot1L contributes to RIPK1 kinase-dependent apoptosis in cerebral ischemia/reperfusion. *J. Am. Heart Assoc.* **2021**, *10*, No. e022791.
(36) Abulafia, D. P.; de Rivero Vaccari, J. P.; Lozano, J. D.; Lotocki, G.; Keane, R. W.; Dietrich, W. D. Inhibition of the inflammasome complex reduces the inflammatory response after thromboembolic stroke in mice. *J. Cereb. Blood Flow Metab.* **2009**, *29*, 534−544.
(37) Mastronardi, C.; Whelan, F.; Yildiz, O. A.; Hannestad, J.; Elashoff, D.; McCann, S. M.; Licinio, J.; Wong, M. L. Caspase 1 deficiency reduces inflammation-induced brain transcription. *Proc. Natl. Acad. Sci. U. S. A.* **2007**, *104*, 7205−7210.

https://doi.org/10.1021/acsmedchemlett.1c00599
ACS Med. Chem. Lett. 2022, 13, 436−442